Calpain inhibition reduces NMDA receptor rundown in rat substantia nigra dopamine neurons

Jerry Zhao[a], Michel Baudry[b] and Susan Jones[a]

[a]Department of Physiology, Development & Neuroscience, University of Cambridge

[b]Graduate College of Biomedical Sciences, Western University of Health Sciences

Address for correspondence:
Dr Sue Jones
Dept of PDN
Downing Street
Cambridge CB2 3DY
sj251@cam.ac.uk

Number of Figures: 5

Key words

Calpain; Dopamine neurons; N-methyl-D-aspartate receptor; Substantia nigra pars compacta

Abstract

Repeated activation of *N*-Methyl-D-aspartate receptors (NMDARs) causes a Ca^{2+}-dependent reduction in NMDAR-mediated current in dopamine (DA) neurons of the substantia nigra pars compacta (SNc) in one week old rats; however, a Ca^{2+}-dependent regulatory protein has not been identified. The role of the Ca^{2+}-dependent cysteine protease, calpain, in mediating NMDAR current rundown was investigated. In brain slices from rats aged postnatal day 7-9 ('P7'), bath application of either of the membrane permeable calpain inhibitors, N-Acetyl-L-leucyl-L-leucyl-L-norleucinal (ALLN, 20 μM) or MDL-28170 (30 μM) significantly reduced whole-cell NMDAR current rundown. To investigate the role of the calpain-2 isoform, the membrane permeable calpain-2 inhibitor, Z-Leu-Abu-CONH-CH2-C6H3 (3, 5-(OMe)2 (C2I, 200 nM), was applied; C2I application significantly reduced whole cell NMDAR current rundown. Interestingly, ALLN but not C2I significantly reduced rundown of NMDA-EPSCs. These results suggest the calpain-2 isoform mediates Ca^{2+}-dependent regulation of extrasynaptic NMDAR current in the first postnatal week, while calpain-1 might mediate rundown of synaptic NMDAR currents. One week later in postnatal development, at P12-P16 ('P14'), there was significantly less rundown in SNc-DA neurons, and no significant effect on rundown of either Ca^{2+} chelation or treatment with the calpain inhibitor, ALLN, suggesting that the rundown observed in SNc-DA neurons from two week-old rats might be Ca^{2+}-independent. In conclusion, Ca^{2+}-dependent rundown of extrasynaptic NMDAR currents in SNc DA neurons involves calpain-2 activation, but Ca^{2+}- and calpain-2-dependent NMDAR current rundown is developmentally regulated.

1. INTRODUCTION

N-Methyl-D-aspartate receptors (NMDARs) are ionotropic glutamate receptors that play important roles in neuronal development and plasticity (Cull-Candy and Leszkiewicz, 2004; Luscher and Malenka, 2012; Paoletti *et al*., 2013; Traynelis *et al*, 2010; Wyllie *et al*., 2012). One important functional feature of NMDARs is their Ca^{2+} permeability, which results in activation of intracellular signalling pathways, including those that promote cell survival (Hardingham and Bading, 2010; Traynelis *et al*., 2010; Vyklicky *et al*., 2014). However, over-activity of NMDARs and the resulting excessive Ca^{2+} influx are also implicated in neuronal dysfunction and excitotoxicity through the activation of cell death signalling pathways (Choi, 1987; Hardingham and Bading, 2010; Surmeier *et al*., 2010). This mechanism could be a contributing factor to neurodegenerative diseases, such as Alzheimer's, Huntington's and Parkinson's diseases (Parsons and Raymond, 2014; Ambrosi *et al*., 2014).

NMDARs are themselves regulated by Ca^{2+}-dependent processes, including a Ca^{2+}-dependent reduction of NMDAR current, termed inactivation or rundown (Ehlers *et al*., 1996; Legendre *et al*., 1993; Rosenmund *et al*., 1995). NMDAR current rundown has previously been shown in substantia nigra pars compacta (SNc) dopaminergic (DA) neurons when NMDA was repetitively applied at an interval less than 400 s (Wild *et al*., 2014). Rundown was dependent on Ca^{2+} influx as it was reduced by increasing the concentration of intracellular buffer (from 0.6 mM EGTA to 10 mM BAPTA), by replacing extracellular Ca^{2+} ions with Ba^{2+} ions, or by reducing the driving force for Ca^{2+} entry by depolarising the membrane potential to +40 mV (Wild et al., 2014). The Ca^{2+}-dependent regulatory mechanism has not been identified. SNc DA neurons form a critical part of the basal ganglia circuitry involved in voluntary motor control (Hegarty *et al*., 2013), and their spiking is strongly influenced by glutamatergic inputs and NMDAR activity (Blythe *et al*., 2007; Jones *et al*., 2011). Degeneration of SNc-DA neurons is a pathological hallmark of Parkinson's disease (Obeso *et al*., 2010; Beitz, 2014), and deregulated Ca^{2+} influx is a possible contributing factor to DA neuronal death (Surmeier *et al*., 2010; 2011). Therefore, there is considerable interest in identifying the factors that regulate NMDAR activity in these and other brain neurons.

Calpain is a Ca^{2+}-dependent cysteine protease, which is activated upon NMDAR stimulation, and calpain is widely expressed in the mammalian central nervous system (Baudry and Bi, 2016). Calpain has been shown to regulate NMDAR activity in synaptic membranes (Bi *et*

al., 1998) and over-activation of NMDARs results in a calpain-dependent suppression of NMDAR currents (Wu *et al.*, 2005). Calpain is also implicated in the pathophysiology of several neurological diseases such as traumatic brain injury and ischemia (Goll et al., 2003; Curcio *et al.*, 2016). While 15 members have been identified in the calpain family (Sorimachi et al., 2010), the two major isoforms expressed in the brain are calpain-1 (μ-calpain) and calpain-2 (m-calpain) (Doshi and Lynch, 2009; Baudry and Bi, 2016). These two isoforms exhibit differing Ca^{2+} sensitivity (micromolar versus milimolar concentrations of Ca^{2+} respectively; Dayton, 1982), and recent studies have suggested that they play opposite functions in synaptic plasticity and neuronal death (Baudry and Bi, 2016). Calpain expression is also isoform-dependent, with calpain-1 being expressed in neuronal somata and calpain-2 expressed in axonal processes and glial cells (Siman et al., 1985). Furthermore, higher levels of calpain are found in hindbrain and midbrain structures compared with forebrain structures in rats (Simonson et al., 1985). Calpain is present in SNc-DA neurons in the adult rat (Siman et al., 1985), although in human post-mortem brains, calpain-2 was detected only in the substantia nigra of Parkinsonian (PD) patients, not in control subjects (Mouatt-Prigent *et al.*, 1996), raising the possibility that calpain-2 might be upregulated in PD. In this study, the role of calpain in Ca^{2+}-dependent NMDAR current rundown in SNc-DA neurons was investigated using two inhibitors that target both of these calpain isoforms (ALLN and MDL-28170) and one inhibitor more selective for the calpain-2 isoform, Z-Leu-Abu-CONH-CH2-C6H3 (3, 5-(OMe)2 (C2I) (Wang et al., 2014), and a significant reduction in NMDAR current rundown was observed.

2. MATERIALS AND METHODS

Wistar rats (Charles River) aged postnatal day 7-16 were used in all experiments in accordance with the Animals (Scientific procedures) Act 1986 and with the University of Cambridge Animal Welfare and Ethical Review Board. Animals were housed in 12 hour light/dark cycle with up to 8 pups per dam and *ad libitum* access to food and water. Rats were anesthetized with isofluorane, then decapitated and brains were removed and submerged in ice-cold solution containing (mM): NaCl 52.5, sucrose 100, KCl 2.5, NaH_2PO_4 1.25, $NaHCO_3$ 26, glucose 25, $MgCl_2$ 5, $CaCl_2$ 1, kynurenic acid 0.1; pH 7.4 with 95% O_2/5% CO_2. Horizontal slices (250 – 300 μm) containing the substantia nigra were made using a Campden 7000smz Vibrating Microtome (Campden Instruments, UK). Slices were then transferred to

an incubation chamber containing (mM): NaCl 119, KCl 2.5, NaH_2PO_4 1.25, $NaHCO_3$ 26, glucose 25, $MgCl_2$ 5, $CaCl_2$ 2 at 30 °C, saturated with 95% O_2 and 5% CO_2, and left undisturbed for 45 minutes to 5 hours.

Brain slices were transferred to a recording chamber and perfused at 2-3mL/min with oxygenated solution (as stated above except with 10 mM glucose and 0.1 mM $MgCl_2$) at 30 ± 2 °C. In some experiments, no $CaCl_2$ was added to the recording solution and instead 2 mM $BaCl_2$ was added (nominally Ca^{2+}-free solution). Patch pipettes with a tip resistance of 1.5-3.5MΩ were filled with intracellular solution containing (mM): $CsMeSO_3$ 120, CsCl 5, NaCl 2.8, 4-(2-hydroxyethyl)-1-piperazineethanesulfonic acid (HEPES) 20, $MgCl_2$ 3, $CaCl_2$ 0.5, Mg-ATP (adenosine triphosphate) 2, Na-GTP (guanine triphosphate) 0.3, Ethylene glycol-bis(2-aminoethylether)-*N,N,N′,N′*-tetraacetic acid (EGTA) 0.6, EGTA 10 or 1,2-Bis(2-aminophenoxy)ethane-N,N,N′,N′-tetraacetic acid tetrakis(acetoxymethyl ester) (BAPTA) 10, as indicated in the text (pH 7.2-3, 270-290 mOsm). Series resistance was measured between each agonist application and was typically 3-5 MΩ; recordings were discarded if the series resistance was unstable. SNc-DA neurons were identified by visually locating the medial terminal nucleus of the accessory optic tract. DA neurons make up ~90% of the SNc neuronal population and exhibit a time-dependent, hyperpolarization-activated inward current (I_h) (of more than 50 pA) following a voltage step from -60 to -120 mV (Margolis *et al*., 2006; Wild et al., 2014; Neuhoff *et al*., 2002; Washio *et al*., 1999).

SNc-DA neurons were voltage clamped to -60 mV, -50 mV or +40 mV (as indicated in the text) using an Axopatch 200B patch clamp amplifier (Molecular Devices, USA). Whole-cell currents were elicited by agonist applications (NMDA 0.5 mM; 5 s in duration; 100 s interval; 10 psi) via a Picospritzer II (General Valve corporation), positioned ~200 μm away from the cell, in the presence of picrotoxin 50 μM, glycine 10 μM and tetrodotoxin (TTX) 100 nM. Application via the picospritzer results in ~50% dilution to ~250 μM NMDA (Wild et al., 2013). Synaptic NMDARs were stimulated using a bipolar stainless steel electrode (Frederick Haer and Co., USA); stimuli (100 μs duration, amplitude 60 to 250 μA) were applied every 10 s in the presence of picrotoxin (50 μM), glycine (10 μM) and DNQX (10 μM). Drugs were applied to the perfusion solution immediately after the visualization of the I_h; the first NMDA application occurred at least 300 s after drug application.

Data were recorded and analysed using Spike 2 software (Version 4; Cambridge Electronic Design, Cambridge, UK). To quantify the extent of rundown, peak current amplitude in response to electrical stimulation or agonist application was measured. The ratio of the average NMDAR-EPSC recorded at 500-600 s to the average NMDAR-EPSC at 0-100 s ($I_{t500\text{-}600s}/I_{t(0\text{-}100s)}$), or the ratio of the last agonist-induced response to the first response (I_{t300}/I_{t0}) was calculated. Statistical analyses were carried out using GraphPad Prism (version 4.0, La Jolla California, USA). Data distribution was assessed using the Shapiro Wilk Normality test. When comparing two groups of paired or unpaired data, the paired or unpaired Student's t-test or a non-parametric test were used. For more than two groups of data, one-way ANOVA with Tukey's post-tests were used. Data are expressed as mean ± standard error (SE), and 'n' values indicate the number of cells, which is equivalent to the number of slices.

3. RESULTS

3.1 Repeated agonist application leads to Ca^{2+}-dependent NMDAR current rundown

NMDAR current rundown was confirmed in SNc-DA neurons from P7-P9 ('P7') rats by four consecutive agonist applications. Neurons were voltage clamped to -60 mV with the Ca^{2+} chelator EGTA (0.6 mM) in the intracellular pipette solution. Under these conditions, the peak inward current decreased in amplitude after the first agonist application (Figure 1A, B, E). The initial current response to NMDA application (I_{t0}) had a mean amplitude of 1657 ± 278 pA, while the fourth response (I_{t300}) was significantly reduced, with a mean amplitude of 785 ± 110 pA (n = 16 cells from 15 rats; P = 0.0005; Wilcoxon signed rank test; Figure 1B). Rundown was not significantly different in the presence of $CdCl_2$ (200 μM; 0.53 ± 0.11, n = 4 cells from 4 rats; P = 0.96, Mann Whitney test), which blocks voltage-gated Ca^{2+} channels (Lansman et al., 1986).

Previously, two mechanisms were suggested to regulate NMDAR rundown in SNc-DA neurons: Ca^{2+}-independent receptor trafficking and an unidentified Ca^{2+}-dependent process (Wild *et al*., 2014). In order to confirm the Ca^{2+}-dependence of rundown, the individual conditions that previously caused a reduction in rundown were combined: DA neurons were voltage-clamped to +40 mV to reduce the driving force for Ca^{2+} influx, EGTA in the intracellular pipette solution was replaced with the more rapid Ca^{2+} chelator BAPTA, at a

higher concentration (10 mM), and extracellular Ca^{2+} was replaced with an equal concentration of Ba^{2+} (nominally Ca^{2+}-free solution). Under these conditions, there was still a significant rundown; mean I_{t0} was 3162 ± 659 pA and mean I_{t300} was 2552 ± 561 pA (Figure 1C, D; n = 7 cells from 7 rats; $t_{(6)} = 3.73$; $P = 0.01$, paired t-test test). However, the extent of rundown was smaller: the ratio of I_{t300} / I_{t0} in Ca^{2+} /EGTA/-60 mV was 0.52 ± 0.04 (n = 16) while in Ba^{2+} /BAPTA/+40 mV, I_{t300}/I_{t0} was 0.8 ± 0.04 (n = 7; $t_{(21)} = 3.97$; $P = 0.0007$, unpaired t- test; Figure 1E). This is in agreement with Wild *et al*. (2014) who showed that NMDAR current rundown is at least partially dependent on an increase in intracellular [Ca^{2+}] due to Ca^{2+} influx. The most likely source of Ca^{2+} influx is via the NMDAR. The difference in rundown between Ca^{2+} /EGTA/-60 mV versus Ba^{2+} /BAPTA/+40 mV could be explained either by the difference in the concentration of Ca^{2+} buffer used, or by the faster kinetics of Ca^{2+} binding to BAPTA as compared with EGTA. To explore this, rundown was measured in recordings in nominally Ca^{2+}-free solution with Ba^{2+} /10 mM EGTA/+40 mV (n = 7 cells from 5 rats); the time course of rundown fell between that for the other two conditions (Figure 1F), suggesting that both the concentration of the buffer and the kinetics of buffering influence Ca^{2+}-dependent rundown.

3.2 Calpain inhibition reduces NMDAR current rundown

Inhibition of Ca^{2+}/calmodulin, α-actinin depolymerisation, or calcineurin did not prevent NMDAR current rundown in SNc-DA neurons (Wild *et al*., 2014). Calpain is another calcium-dependent signalling molecule that has been shown to modulate NMDAR current rundown in cortical neurons (Bi *et al*., 2000, 1998; Wu *et al*., 2005). To investigate whether calpain mediates Ca^{2+}-dependent NMDAR current rundown in SNc-DA neurons, the membrane permeable calpain inhibitor N-Acetyl-L-leucyl-L-leucyl-L-norleucinal (ALLN, 20 μM) was applied to the perfusion solution during recordings (Figure 2A, B, D). The mean I_{t0} in the presence of ALLN was 1229 ± 130 pA, while the mean I_{t300} was 1075 ± 185 pA (n = 9 cells from 7 rats); there was no significant difference between I_{t0} and I_{t300} in ALLN ($t_{(8)}$ = 1.44; $P = 0.19$, paired t-test). There was an overall significant effect of ALLN treatment on the extent of NMDAR current rundown ($F_{(2, 30)} = 7.99$; $P = 0.0017$; one way ANOVA); post-hoc comparisons showed that there was significantly less rundown in ALLN (average I_{t300}/I_{t0} = 0.85 ± 0.09; n = 9) compared to the DMSO vehicle (2:1000; I_{t300}/I_{t0} = 0.50 ± 0.07; n = 8 cells from 5 rats; $P < 0.001$, Tukey's Multiple Comparison test; Figure 2E). The time of the first application of NMDA was 458 ± 53 s after forming the whole-cell configuration, which was not significantly different to the time of the first response in control recordings (465 ±

78, n = 16; $P = 0.95$, unpaired t-test). There was no significant effect of DMSO alone on rundown ($P > 0.05$, Tukey's Multiple Comparison test; Figure 2E).

Application of a second membrane permeable calpain inhibitor, MDL-28170 (30 µM) had an overall significant effect on rundown ($F_{(2, 29)} = 4.72$; $P = 0.017$; one-way ANOVA; Figure 2C, D, F). Post-hoc comparisons showed that rundown was significantly reduced in MDL-28170 ($I_{t300}/I_{t0} = 0.76 \pm 0.1$; n = 9 cells from 6 rats) compared to application of vehicle solution (3:1000 DMSO; $I_{t300}/I_{t0} = 0.47 \pm 0.05$; n = 7 cells from 6 rats; $P < 0.05$, Tukey's Multiple Comparison test). The time of the first application of NMDA was 640 ± 34 s after forming the whole-cell configuration, which was not significantly different to the time of the first response in control recordings (465 ± 78, n = 16; $P = 0.12$, unpaired t-test).

3.3 Calpain-2 inhibition reduces NMDAR current rundown

Two calpain isoforms (calpain-1 and calpain-2) are ubiquitously expressed in the mammalian brain (Doshi and Lynch, 2009; Baudry and Bi, 2016). To investigate which calpain isoform might be responsible for Ca^{2+}-dependent NMDAR current rundown, a membrane permeable inhibitor selective for calpain-2 (Z-Leu-Abu-CONH-CH_2-C_6H_3(3,5-$(OMe)_2$) or C2I, 200 nM) was applied. The mean I_{t0} in the presence of C2I (200 nM) was 1238 ± 222 pA, while the mean I_{t300} was 836 ± 202 pA (n = 11 cells from 9 rats; Figure 3A, B); there was no significant difference between I_{t0} and I_{t300} ($t_{(10)} = 1.52$; $P = 0.32$, paired t-test). There was an overall significant effect of C2I treatment on the extent of NMDAR current rundown ($F_{(2,32)} = 6.94$; $P = 0.003$; one way ANOVA); post-hoc comparisons showed that there was significantly less rundown in C2I (average $I_{t300}/I_{t0} = 0.90 \pm 0.12$; n = 11) compared to the DMSO vehicle (2:1000; $I_{t300}/I_{t0} = 0.50 \pm 0.07$; n = 8 cells from 5 rats; $P < 0.001$, Tukey's Multiple Comparison test; Figure 3D). The time of the first application of NMDA was 564 ± 27 s after forming the whole-cell configuration, which was not significantly different to the time of the first response in control recordings (465 ± 78; $P = 0.32$, unpaired t-test). This finding suggests that the Ca^{2+}-dependent rundown of whole-cell NMDARs in SNc-DA neurons from P7 rats is mediated by calpain-2.

3.4 Ca^{2+}- and calpain-dependent NMDAR current rundown is developmentally regulated

To determine whether rundown is developmentally regulated, experiments were carried out in SNc-DA neurons from rats aged P12-P16 ('P14'). Significant rundown was observed in SNc-DA neurons from P14 rats in Ca/EGTA/-60mV (from 1722 ± 256 pA at I_{t0} to 1071 ± 88 pA at I_{t300}; n = 14 cells from 12 rats; $t_{(13)} = 3.1$; $P = 0.0006$; paired t-test; example shown in Figure

4A). However, the extent of rundown was significantly less than that seen in SNc-DA neurons from P7 rats (Figure 4B; $t_{(28)} = 2.64$; $P = 0.014$, unpaired t-test). In SNc-DA neurons from P14 rats, there was no significant effect of replacing Ca^{2+} /EGTA/-60mV with Ba^{2+} /BAPTA/+40mV (n = 6 cells from 6 rats; $t_{(18)} = 0.97$; $P = 0.34$, unpaired t-test; Figure 4C). Concomitantly, ALLN (20 μM; n = 5 cells from 5 rats) had no significant effect on NMDAR current rundown in SNc-DA neurons from P14 rats ($t_{(17)} = 0.123$; $P = 0.90$, unpaired t-test; Figure 4D, E). These results suggest that Ca^{2+}- and calpain-dependent NMDAR current rundown is developmentally regulated between the first and second postnatal week.

3.5 Calpain inhibition reduces synaptic NMDAR current rundown

NMDAR-EPSCs in SNc-DA neurons were previously shown to rundown over a similar time course to whole-cell NMDAR current rundown (Wild et al., 2014). To determine whether rundown of synaptic NMDARs is also regulated by calpain, NMDAR-EPSCs were recorded at -50 mV in 0.1 mM $MgCl_2$, 50 μM picrotoxin, 10 μM glycine and 10 μM DNQX, using 0.6 mM EGTA as the Ca^{2+} chelator and Ca^{2+} as the charge carrier. In control recordings, the NMDAR-EPSC mean amplitude at $t_{0\text{-}100s}$ was -40 ± 11.6 pA (n = 7 cells from 7 rats); this was significantly reduced at $t_{500\text{-}600s}$ (22.4 ± 8.2 pA, n = 7; $t_{(6)} = 3.35$; $P = 0.015$, paired t-test; Figure 5A, B). In the presence of ALLN (20 μM), NMDAR-EPSC mean amplitude at $t_{0\text{-}100s}$ was -34.5 ± 5.2 pA (n = 7 cells from 7 rats); this was not significantly different at $t_{500\text{-}600s}$ (35.1 ± 6.0 pA, n = 7; P = 0.94, Wilcoxon signed rank test; Figure 5C, D). In the presence of C2I (200 nM), the mean NMDAR-EPSC amplitude at $t_{0\text{-}100s}$ was -30.6 ± 4.1 pA (n = 7 cells from 7 rats); this was significantly reduced at $t_{500\text{-}600s}$ (18.1 ± 2.3 pA, n = 7; $t_{(6)} = 5.16$; $P = 0.002$, paired t-test). The time course of NMDAR-EPSC rundown in control, DMSO (2/1000), ALLN and C2I is shown in Figure 5E. Rundown, quantified as the ratio of $t_{500\text{-}600s}/t_{0\text{-}100s}$ (Figure 5F), was significantly less in ALLN (1.0 ± 0.06) than in control (0.54 ± 0.11; P < 0.01), C2I (0.61 ± 0.04; P < 0.05), or DMSO (0.67 ± 0.1; P < 0.05); Tukey's Multiple Comparisons test following one way ANOVA ($F_{(3, 28)} = 5.9$; $P = 0.003$). These results suggest that calpain-1 activation but not calpain-2 activation participates in rundown of synaptic NMDAR currents.

4. DISCUSSION

Activity- and Ca^{2+}-dependent regulation, such as rundown of NMDAR currents is a potential mechanism to limit excessive Ca^{2+} influx and might serve a neuroprotective role under

excitotoxic conditions. Several regulatory mechanisms responsible for Ca^{2+}-dependent NMDAR current rundown have been identified in hippocampal and cortical neurons. NMDARs can bind signal transduction molecules via the C-termini of their subunits and this can alter NMDAR number, distribution and activity at the plasma membrane (Lin *et al*., 2004; Petralia *et al*., 2009; Salter *et al*., 2009). Ca^{2+}-dependent proteins regulating NMDARs include serine/ threonine kinases and phosphatases; for example, application of Ca^{2+} and CaM reduced single channel activity in HEK cells expressing GluN1/GluN2A receptors (Krupp *et al*., 1999). However, in SNc-DA neurons, inhibitors of serine/ threonine kinases and phosphatases had no effect on NMDAR current rundown (Wild *et al*., 2014).

Another Ca^{2+}-dependent mechanism regulating receptor function consists of the activation of calpain, a Ca^{2+}-dependent cysteine protease. Calpain is activated by NMDAR-mediated Ca^{2+} influx and can in turn regulate NMDAR activity (Bi *et al.*, 1998; Wu *et al.*, 2005). Whole-cell NMDAR current rundown in SNc-DA neurons was reduced in the presence of two broad spectrum calpain inhibitors (ALLN and MDL-28170) and by a more selective inhibitor of the calpain-2 isoform, implicating calpain-2 as the Ca^{2+}-dependent mechanism involved in whole-cell NMDAR current rundown in SNc-DA neurons. Interestingly, synaptic NMDAR rundown was also reduced by the broad spectrum calpain inhibitor, ALLN, but not by the calpain-2 inhibitor. Extrasynaptic NMDAR currents are more likely to be assessed in whole-cell recording, suggesting that different calpain isoforms regulate rundown of synaptic versus extrasynaptic NMDAR currents. Extrasynaptic NMDAR stimulation could lead to calpain-2 activation through the stimulation of ERK and the phosphorylation of Ser 50 of calpain-2 (Baudry and Bi, 2016). In contrast, it was previously shown that activation of synaptic NMDARs, but not extrasynaptic NMDARs results in recruiting of calpain-1 to NMDARs (Wang et al., 2013). This could account for the selective rundown of synaptic NMDARs by calpain-1. As increased levels of calpain-2 have specifically been associated with SNc-DA neurons exhibiting pathology in post-mortem brains of PD but not control patients (Mouatt-Prigent *et al*., 1996), it is possible that increased calpain-2 expression represents a neuroprotective mechanism to autoregulate extracellular NMDAR-mediated Ca^{2+} influx when this becomes pathologically high.

Although calpain activity resulted in reduced NMDAR current, rundown was not completely blocked by calpain inhibition. It is possible that other Ca^{2+}-binding proteins contribute to rundown, alongside calpain. For example, calbindin inhibits Ca^{2+}-dependent rundown of

NMDARs expressed in HEK-293 cells (Price *et al*., 1999). However, the remaining rundown is likely to be Ca^{2+}-independent, as dynamin inhibition has been shown to block a component of rundown in SNc-DA neurons (Wild *et al*., 2014). Ca^{2+}-independent rundown is also likely to account for the rundown observed during recordings at +40 mV, to reduce the driving force for Ca^{2+} influx, and in nominally Ca^{2+}-free solution (using Ba^{2+} as the charge carrier), with either 10 mM EGTA or 10 mM BAPTA. Some Ca^{2+} influx may still occur under these conditions, but the rundown of 20-30% seen under these conditions is consistent with the Ca^{2+}-independent rundown reported by Wild *et al*. (2014).

What might be the downstream mechanism by which calpain effects rundown? Studies have shown that the C-terminal domains (CTD) of NMDARs may be important, as deletion of the GluN1 CTD eliminates Ca^{2+}-dependent NMDAR inactivation (Ehlers *et al*., 1996). Calpains have been shown to interact directly with NMDARs and cleave the CTD of GluN2A, 2B, and 2C subunits (Doshi and Lynch, 2010; Guttmann et al., 2001). It is possible that a similar mechanism exists in SNc-DA neurons, such that the proteolysis of NMDAR subunits by calpain could result in decreased NMDAR activity and/or decreased NMDAR surface expression, thereby reducing currents from subsequent NMDAR stimulation. This hypothesis could account for the lack of reversibility of the NMDAR rundown (Wild et al, 2014). Evidence suggests that GluN2A subunits do not contribute to functional synaptic or extrasynaptic NMDARs in postnatal SNc-DA neurons (Brothwell *et al*., 2008; Jones and Gibb, 2005; Suarez *et al*., 2010) and GluN2C subunits are not expressed at detectable levels (Hallett and Standaert, 2004). However, calpains have been shown to exhibit selectivity in the degradation of GluN2B over GluN2A subunits (Araújo *et al*., 2005; Simpkins *et al*., 2003). It was previously shown that, after inhibiting the GluN2B component of whole-cell NMDAR current using ifenprodil, the remaining component (presumed to be GluN2D-mediated) does not show Ca^{2+}-dependent rundown (Wild *et al*., 2014). Therefore, it is likely that in SNc-DA neurons calpain would act on GluN2B subunits. Interestingly, neighbouring DA neurons of the ventral tegmental area (VTA) express GluN2A as well as GluN2B subunits (Borgland *et al*., 2006); as VTA DA neurons also express calpain (Liu *et al*., 2007; Mouatt-Prigent *et al*., 1996), it is likely that NMDARs in VTA DA neurons are a target for Ca^{2+}- and calpain-dependent regulation. It would be interesting to compare calpain regulation of NMDARs and its potential neuroprotective role in VTA versus SNc DA neurons.

Studies on substrates specific for the two major calpain isoforms (calpain-1 and calpain-2) are scarce, but calpain-1 and calpain-2 have different PDZ binding motifs and have been suggested to associate with distinct protein clusters (Baudry and Bi, 2016). For example, it has been shown that calpain-1 selectively associates with NMDAR multiprotein complexes and co-immunoprecipitates with PSD-95 and GluN2A subunits after synaptic activation (Wang et al., 2013). This finding supports the idea that calpain-1 is generally associated with synaptic NMDARs, and the lack of effect of calpain-2 inhibition on NMDA-EPSCs would support this idea. On the other hand, NR2B subunits directly bind RasGRF1, which provides a link between NMDAR activation and ERK (Krapivinsky et al., 2003), and the resulting calpain-2 activation. Inhibition of calpain-2 reduced striatal enriched protein tyrosine phosphatase 61 ($STEP_{61}$) cleavage and cell death after extrasynaptic NMDAR activation (Wang *et al*., 2013). Therefore, calpain-2-mediated regulation of extrasynaptic NMDAR rundown in SNc-DA neurons could represent a negative feed-back providing a neuroprotective process under excitotoxic conditions.

NMDARs of SNc-DA neurons are proposed to undergo a developmental transition from GluN1/GluN2B and GluN1/GluN2D-containing diheteromeric receptors to GluN1/ GluN2B/ GluN2D containing triheteromeric receptors (Brothwell *et al*., 2008; Suárez *et al*., 2010). This transition occurs between P7 and P14 and affects receptor properties such as decay kinetics and sensitivity to Mg^{2+} block. NMDAR current rundown was measured during the second week of postnatal development, and was present but reduced in amplitude, as compared with the first postnatal week. This seems likely to be due to a reduction of Ca^{2+}- and calpain-dependent rundown, as conditions to minimise an increase in intracellular Ca^{2+} or to inhibit calpain activity had no significant effect on rundown in slices from P14 rats. It is plausible that calpain activity is reduced between P7 and P14, as a decrease in calpain-2 activity has been reported during postnatal development (Simonson et al., 1985). This raises the interesting possibility that calpain-2 is down-regulated during postnatal development, but up-regulated under various pathological conditions, including PD (Mouatt-Prigent *et al*., 1996). Alternatively, a change in NMDAR subunit composition between P7 and P14, from predominantly GluN1/GluN2B and GluN1/GluN2D diheteromeric receptors to putative GluN1/GluN2B/GluN2D triheteromeric receptors (Brothwell *et al*., 2008; Suarez *et al*., 2010), may render NMDAR less susceptible to current rundown; in support of this, there was significantly less rundown of the ifenprodil-insensitive NMDAR current (Wild *et al*., 2014). These are all important considerations, as developing SNc-DA neurons may be losing a

neuroprotective effect provided by calpain-2 and may as a result become more vulnerable to excitotoxic insult. However, the possibility that both Ca^{2+}-dependent and Ca^{2+}-independent rundown were concurrently reduced during early postnatal development, rather than a specific reduction only in Ca^{2+}-dependent rundown, cannot currently be ruled out.

In conclusion, these results implicate calpain-2 in the Ca^{2+}-dependent regulation of extrasynaptic NMDARs and calpain-1 in the Ca^{2+}-dependent regulation of synaptic NMDARs in SNc-DA neurons during the first postnatal week and suggest that these roles of calpain-1 and calpain-2 are developmentally regulated.

Acknowledgements

We thank Professor Giles Hardingham for suggesting calpain as a possible mediator of NMDAR rundown in SNc-DA neurons. No grant funding was received for this study.

Figure legends

Figure 1: Repeated agonist application induces Ca^{2+}-dependent NMDAR current rundown in P7 rats

A. Example current recorded from a SNc-DA neuron voltage-clamped to -60 mV with 0.6 mM EGTA in the intracellular solution. NMDA was applied for 5 s at 100 s intervals (arrows). Deflections in the trace indicates series resistance checks. B. Graph showing the initial (t_{0s}) and final (t_{300s}) current amplitude for all experiments in Ca/EGTA/-60mV (n = 16; ***P = 0.0005, Wilcoxon signed rank test). C. Example current recorded from a SNc-DA neuron voltage-clamped to +40 mV with Ca^{2+} replaced by Ba^{2+} in the extracellular solution and 10 mM BAPTA in the intracellular solution. D. Graph showing the initial (t_{0s}) and final (t_{300s}) current amplitude for all experiments in Ba/ BAPTA/ +40mV (n = 7; P = 0.01, paired t-test). E. Rundown was significantly less in Ba/ 10 mM BAPTA/ +40mV than in Ca/ 0.6 mM EGTA/ -60mV. ***P = 0.007, paired t-test. F. Time-course of rundown with either Ca/0.6mM EGTA/-60mV, Ba/10mM EGTA/+40mV or Ba/10mM BAPTA/+40mV.

Figure 2: Calpain inhibition reduces NMDAR current rundown in P7 rats

A. Example current recorded from a SNc-DA neuron voltage-clamped to -60 mV with 0.6 mM EGTA in the intracellular solution and ALLN (20 μM) in the perfusion. NMDA was applied for 5 s at 100 s intervals (arrows). B. Graph showing the amplitude of NMDAR currents at t_{0s} and t_{300s} for all experiments recorded in ALLN (n = 9; P = 0.19). C. Example current recorded from a SNc-DA neuron voltage-clamped to -60 mV with 0.6 mM EGTA in the intracellular solution and MDL-28170 (30 μM) in the perfusion. NMDA was applied for 5 s at 100 s intervals (arrows). D. Time course of rundown with either control, DMSO, ALLN or MDL in the perfusion (Ca/0.6 EGTA/-60mV). E. Comparison of initial and final mean current amplitude in DMSO (n = 8), control (n = 16) or ALLN (n = 9; **P < 0.01, Tukey's Multiple Comparison test). F. Comparison of initial and final mean current amplitude in DMSO (n = 7), control (n = 16) and MDL (n = 9). *P < 0.05, Tukey's Multiple Comparison test.

Figure 3: Calpain-2 inhibition reduces rundown in P7 rats

A. Example current recorded from a SNc-DA neuron voltage-clamped to -60 mV with 0.6 mM EGTA in the intracellular solution and calpain-2 inhibitor (C2I, 200 nM) in the perfusion. NMDA was applied for 5 s at 100 s intervals (arrows). B. Graph showing the amplitude of NMDAR currents at t_{0s} and t_{300s} for all experiments recorded in C2I (n = 11; *P* = 0.16). C. Time course of rundown in control, DMSO (2/1000) or C2I. D. Comparison of initial and final mean current amplitude in control (n = 16), DMSO (n = 8) or C2I (n = 9). **P* < 0.05, ***P* < 0.01, Tukey's Multiple Comparison test.

Figure 4: Ca^{2+}- and calpain-dependent NMDAR current rundown in P14 rats

A. Example current recorded from a SNc-DA neuron voltage-clamped to -60 mV with 0.6 mM EGTA in the intracellular solution. NMDA was applied for 5 s at 100 s intervals (arrows). B. There was significantly less NMDAR current rundown in SNc-DA neurons from P14 rats compared with P7 rats (in Ca/EGTA/-60mV; **P* = 0.014, unpaired t-test). C. There was no significant difference in rundown in Ba/ BAPTA/+40mV (n = 6) compared with Ca/ EGTA/-60mV (n = 14) in P14 animals (*P* = 0.35, unpaired t-test). D. Example current recorded from a SNc-DA neuron voltage-clamped to -60 mV with 0.6 mM EGTA in the intracellular solution and ALLN (20 μM) in the perfusion. NMDA was applied for 5 s at 100 s intervals (arrows). E. Application of ALLN (n = 5) had no significant effect on NMDAR current rundown at P14 compared with control (n = 14; *P* = 0.90, unpaired t-test).

Figure 5: Calpain inhibition reduces synaptic NMDAR current rundown in P7 rats

A. Example NMDAR-EPSCs recorded from a SNc-DA neuron voltage-clamped to -50 mV with 0.6 mM EGTA in the intracellular solution. B. Graph showing the initial ($t_{0\text{-}100s}$) and final ($t_{500\text{-}600s}$) NMDAR-EPSC mean amplitude for all experiments in Ca/EGTA/-60mV (n = 7; **P* = 0.015, paired t-test). C. Example NMDAR-EPSCs recorded from a SNc-DA neuron voltage-clamped to -50 mV with 0.6 mM EGTA in the intracellular solution and ALLN (20 μM) in the perfusion. D. Graph showing the initial ($t_{0\text{-}100s}$) and final ($t_{500\text{-}600s}$) NMDAR-EPSC amplitude for all experiments in Ca/EGTA/-60mV with ALLN in the perfusion (n = 7; *P* = 0.93, Wilcoxon signed rank test). E. Example NMDAR-EPSCs recorded from a SNc-DA neuron voltage-clamped to -50 mV with 0.6 mM EGTA in the intracellular solution and C2I

(200 nM) in the perfusion. F. Graph showing the initial ($t_{0\text{-}100s}$) and final ($t_{500\text{-}600s}$) NMDAR-EPSC amplitude for all experiments in Ca/EGTA/-60mV with C2I in the perfusion (n = 7; *P* = 0.002, paired t-test). G. Time-course of NMDAR-EPSC rundown with either control, DMSO (2/1000), ALLN (20 μM) or C2I (200 nM). H. Rundown was significantly less in ALLN than in control (***P* < 0.01) or DMSO/ C2I (**P* < 0.05; ANOVA and Tukey's Multiple Comparison test).

References

Ambrosi G, Cerri S, Blandini F (2014). A further update on the role of excitotoxicity in the pathogenesis of Parkinson's disease. J Neural Transm *121*:849-59.
DOI: 10.1007/s00702-013-1149-z

Araújo, I.M., Xapelli, S., Gil, J.M.A.C., Mohapel, P., Petersén, A., Pinheiro, P.S., Malva, J.O., Bahr, B.A., Brundin, P., and Carvalho, C.M. (2005). Proteolysis of NR2B by calpain in the hippocampus of epileptic rats. Neuroreport *16*, 393–396.

Baudry, M., and Bi, X. (2016). Calpain-1 and Calpain-2: The yin and yang of synaptic plasticity and neurodegeneration. Trends Neurosci. *39*, 235–245.
DOI: 10.1016/j.tins.2016.01.007

Beitz, J.M. (2014). Parkinson's disease: a review. Front. Biosci. Sch. Ed. *6*, 65–74.
Bi, R., Rong, Y., Bernard, A., Khrestchatisky, M., and Baudry, M. (2000). Src-mediated tyrosine phosphorylation of NR2 subunits of N-Methyl-d-Aspartate receptors protects from calpain-mediated truncation of their C-terminal domains. J. Biol. Chem. *275*, 26477–26483.
DOI: 10.1074/jbc.M003763200

Bi, X., Rong, Y., Chen, J., Dang, S., Wang, Z., and Baudry, M. (1998). Calpain-mediated regulation of NMDA receptor structure and function. Brain Res. *790*, 245–253.

Blythe SN1, Atherton JF, Bevan MD (2007). Synaptic activation of dendritic AMPA and NMDA receptors generates transient high-frequency firing in substantia nigra dopamine neurons in vitro. J Neurophysiol. *97*:2837-50.
DOI: 10.1152/jn.01157.2006

Borgland, S.L., Taha, S.A., Sarti, F, Fields, H.L., Bonci, A. (2006). Orexin A in the VTA Is Critical for the Induction of Synaptic Plasticity and Behavioral Sensitization to Cocaine. Neuron 49:589-681.
DOI: https://doi.org/10.1016/j.neuron.2006.01.016

Brothwell, S.L.C., Barber, J.L., Monaghan, D.T., Jane, D.E., Gibb, A.J., and Jones, S. (2008). NR2B- and NR2D-containing synaptic NMDA receptors in developing rat substantia nigra pars compacta dopaminergic neurones. J. Physiol. *586*, 739–750.
DOI: 10.1113/jphysiol.2007.144618

Choi, D.W. (1987). Ionic dependence of glutamate neurotoxicity. J. Neurosci. *7*, 369–379.

Cull-Candy, S.G., and Leszkiewicz, D.N. (2004). Role of distinct NMDA receptor subtypes at central synapses. Sci STKE *2004*, re16-re16.
DOI: 10.1126/stke.2552004re16

Curcio, M., Salazar, I.L., Mele, M., Canzoniero, L.M.T., and Duarte, C.B. (2016). Calpains and neuronal damage in the ischemic brain: The swiss knife in synaptic injury. Prog. Neurobiol. *143*, 1–35.
DOI: 10.1016/j.pneurobio.2016.06.001

Dayton, W.R. (1982). Comparison of low- and high-calcium-requiring forms of the calcium-activated protease with their autocatalytic breakdown products. Biochim. Biophys. Acta *709*, 166–172.

Doshi, S., and Lynch, D.R. (2009). Calpain and the glutamatergic synapse. Front. Biosci. Sch. Ed. *1*, 466–476.

Ehlers, M.D., Zhang, S., Bernhardt, J.P., and Huganir, R.L. (1996). Inactivation of NMDA receptors by direct interaction of calmodulin with the NR1 subunit. Cell *84*, 745– 755.

Goll, D.E., Thompson, V.F., Li, H., Wei, W., and Cong, J. (2003a). The calpain system. Physiol. Rev. *83*, 731–801.
DOI: 10.1152/physrev.00029.2002

Goto, K., Iwamoto, T., and Kondo, H. (1994). Localization of mRNAs for calpain and calpastatin in the adult rat brain by in situ hybridization histochemistry. Mol. Brain Res. *23*, 40–46.

Guttmann, R.P., Rodney, P., Baker, D.L., Seifert, K.M., Cohen, A.S., Coulter, D.A. and Lynch, D.R. (2001). Specific proteolysis of the NR2 subunit at multiple sites by calpain. J. Neurochem. *78*, 1083-1093.

Hallett, P.J., and Standaert, D.G. (2004). Rationale for and use of NMDA receptor antagonists in Parkinson's disease. Pharmacol. Ther. *102*, 155–174.
DOI: 10.1016/j.pharmthera.2004.04.001

Hardingham, G.E., and Bading, H. (2010). Synaptic versus extrasynaptic NMDA receptor signalling: implications for neurodegenerative disorders. Nat. Rev. Neurosci. *11*, 682–696.
DOI: 10.1038/nrn2911

Hegarty, S.V., Sullivan, A.M., and O'Keeffe, G.W. (2013). Midbrain dopaminergic neurons: a review of the molecular circuitry that regulates their development. Dev. Biol. *379*, 123–138.
DOI: 10.1016/j.ydbio.2013.04.014

Jones, S., and Gibb, A.J. (2005). Functional NR2B- and NR2D-containing NMDA receptor channels in rat substantia nigra dopaminergic neurones. J. Physiol. *569*, 209–221.
DOI: 10.1113/jphysiol.2005.095554

Jones, S., Brothwell, S.L.C., Huang-Doran, I. and Hallett, J. (2011). Ionotropic glutamate receptors in the basal ganglia. In: Frontiers in Neuroscience series, Editor S. Jones, Taylor & Francis / CRC Press

Krapivinsky G.1., Krapivinsky L., Manasian Y., Ivanov A., Tyzio R., Pellegrino C., Ben-Ari Y., Clapham D.E., Medina I. (2003). The NMDA receptor is coupled to the ERK pathway by a direct interaction between NR2B and RasGRF1. Neuron 40:775-784

Krupp, J.J., Vissel, B., Thomas, C.G., Heinemann, S.F., and Westbrook, G.L. (1999). Interactions of calmodulin and α-actinin with the NR1 subunit modulate Ca2+-dependent inactivation of NMDA Receptors. J. Neurosci. *19*, 1165–1178.

Lansman, J.B, Hess, P. and Tsien R.W. (1986). Blockade of Current through Single Calcium Channels by Cd^{2+}, Mg^{2+}, and Ca^{2+}. J. Gen. Physiol. 88:321-347.

Legendre, P., Rosenmund, C., and Westbrook, G.L. (1993). Inactivation of NMDA channels in cultured hippocampal neurons by intracellular calcium. J. Neurosci. *13*, 674–684.

Lin, Y., Skeberdis, V.A., Francesconi, A., Bennett, M.V.L., and Zukin, R.S. (2004). Postsynaptic density protein-95 regulates NMDA channel gating and surface expression. J. Neurosci. *24*, 10138–10148.
DOI: 10.1523/JNEUROSCI.3159-04.2004

Liu Y., Dore J., and Chen, X. (2007). Calcium Influx through L-type Channels Generates Protein Kinase M to Induce Burst Firing of Dopamine Cells in the Rat Ventral Tegmental Area. J Biol Chem 282:8594–8603.
DOI 10.1074/jbc.M610230200

Lüscher, C., and Malenka, R.C. (2012). NMDA receptor-dependent long-term potentiation and long-term depression (LTP/LTD). Cold Spring Harb. Perspect. Biol. *4*.
DOI: 10.1101/cshperspect.a005710

Margolis, E.B., Lock, H., Hjelmstad, G.O., and Fields, H.L. (2006). The ventral tegmental area revisited: is there an electrophysiological marker for dopaminergic neurons? J. Physiol. *577*, 907–924.
DOI: 10.1113/jphysiol.2006.117069

Milnerwood, A.J., and Raymond, L.A. (2010). Early synaptic pathophysiology in neurodegeneration: insights from Huntington's disease. Trends Neurosci. *33*, 513–523.
DOI: 10.1016/j.tins.2010.08.002

Mouatt-Prigent, A., Karlsson, J.O., Agid, Y., and Hirsch, E.C. (1996). Increased m-calpain expression in the mesencephalon of patients with parkinson's disease but not in other neurodegenerative disorders involving the mesencephalon: a role in nerve cell death? Neuroscience *73*, 979–987.

Neuhoff, H., Neu, A., Liss, B., and Roeper, J. (2002). Channels contribute to the different functional properties of identified dopaminergic subpopulations in the midbrain. J. Neurosci. *22*, 1290–1302.

Obeso, J.A., Rodriguez-Oroz, M.C., Goetz, C.G., Marin, C., Kordower, J.H., Rodriguez, M., Hirsch, E.C., Farrer, M., Schapira, A.H.V., and Halliday, G. (2010). Missing pieces in the Parkinson's disease puzzle. Nat. Med. *16*, 653–661.
DOI: 10.1038/nm.2165

Paoletti, P., Bellone, C., and Zhou, Q. (2013). NMDA receptor subunit diversity: impact on receptor properties, synaptic plasticity and disease. Nat. Rev. Neurosci. *14*, 383–400.
DOI: 10.1038/nrn3504

Parsons MP, Raymond LA (2014). Extrasynaptic NMDA receptor involvement in central nervous system disorders. Neuron. *82*:279-93.
DOI: 10.1016/j.neuron.2014.03.030

Petralia, R.S., Al-Hallaq, R.A., and Wenthold, R.J. (2009). Trafficking and targeting of NMDA receptors. In biology of the NMDA receptor, A.M. Van Dongen, ed. (Boca Raton (FL): CRC Press/Taylor & Francis).

Price, C.J., Rintoul, G.L., Baimbridge, K.G., and Raymond, L.A. (1999). Inhibition of calcium-dependent NMDA receptor current rundown by calbindin-D28k. J. Neurochem. *72*, 634–642.

Rosenmund, C., and Westbrook, G.L. (1993). Calcium-induced actin depolymerization reduces NMDA channel activity. Neuron *10*, 805–814.

Rosenmund, C., Feltz, A., and Westbrook, G.L. (1995). Calcium-dependent inactivation of synaptic NMDA receptors in hippocampal neurons. J. Neurophysiol. *73*, 427–430.
DOI: 10.1152/jn.1995.73.1.427

Rycroft, B.K., and Gibb, A.J. (2002). Direct effects of calmodulin on NMDA receptor single-channel gating in rat hippocampal granule cells. J. Neurosci. *22*, 8860–8868.

Rycroft, B.K., and Gibb, A.J. (2004). Inhibitory interactions of calcineurin (phosphatase 2B) and calmodulin on rat hippocampal NMDA receptors. Neuropharmacology *47*, 505–514.
DOI: 10.1016/j.neuropharm.2004.06.001

Salter, M.W., Dong, Y., Kalia, L.V., Liu, X.J., and Pitcher, G. (2009). Regulation of NMDA receptors by kinases and phosphatases. In biology of the NMDA receptor, A.M. Van Dongen, ed. (Boca Raton (FL): CRC Press/Taylor & Francis).

Samantaray, S., Knaryan, V.H., Shields, D.C., Cox, A.A., Haque, A., and Banik, N.L. (2015). Inhibition of calpain activation protects MPTP-induced nigral and spinal cord neurodegeneration, reduces inflammation, and improves gait dynamics in mice. Mol. Neurobiol. *52*, 1054–1066.
DOI: 10.1007/s12035-015-9255-6

Siman, R., Gall, C., Perlmutter, L.S., Christian, C., Baudry, M., and Lynch, G. (1985). Distribution of calpain I, an enzyme associated with degenerative activity, in rat brain. Brain Res. *347*, 399–403.

Simonson, L., Baudry, M., Siman, R. and Lynch, G. (1985). Regional distribution of soluble calcium activated proteinase activity in neonatal and adult rat brain. Brain Res. *327*, 153-159.

Simpkins, K.L., Guttmann, R.P., Dong, Y., Chen, Z., Sokol, S., Neumar, R.W., and Lynch, D.R. (2003). Selective activation induced cleavage of the NR2B subunit by calpain. J. Neurosci. *23*, 11322–11331.

Suárez, F., Zhao, Q., Monaghan, D.T., Jane, D.E., Jones, S., and Gibb, A.J. (2010). Functional heterogeneity of NMDA receptors in rat substantia nigra pars compacta and reticulata neurones. Eur. J. Neurosci. *32*, 359–367.
DOI: 10.1111/j.1460-9568.2010.07298.x

Surmeier, D.J., Guzman, J.N., and Sanchez-Padilla, J. (2010). Calcium, cellular aging, and selective neuronal vulnerability in Parkinson's disease. Cell Calcium *47*, 175–182.
DOI: 10.1016/j.ceca.2009.12.003

Surmeier, D.J., Guzman, J.N., Sanchez-Padilla, J., and Schumacker, P.T. (2011). The role of calcium and mitochondrial oxidant stress in the loss of substantia nigra pars compacta dopaminergic neurons in Parkinson's disease. Neuroscience *198*, 221–231.
DOI: 10.1016/j.neuroscience.2011.08.045

Sorimachi H., Hata S., Ono Y. (2010). Expanding members and roles of the calpain superfamily and their genetically modified animals. Exp Anim. 59:549-66.

Traynelis, S.F., Wollmuth, L.P., McBain, C.J., Menniti, F.S., Vance, K.M., Ogden, K.K., Hansen, K.B., Yuan, H., Myers, S.J., and Dingledine, R. (2010). Glutamate receptor ion channels: structure, regulation, and function. Pharmacol. Rev. *62*, 405–496.
DOI: 10.1124/pr.109.002451

Vyklicky, V., Korinek, M., Smejkalova, T., Balik, A., Krausova, B., Kaniakova, M., Lichnerova, K., Cerny, J., Krusek, J., Dittert, I., et al. (2014). Structure, function, and pharmacology of NMDA receptor channels. Physiol. Res. *63 Suppl 1*, S191-203.

Wang, Y., Briz, V., Chishti, A., Bi, X., and Baudry, M. (2013). Distinct roles for μ-calpain and m-calpain in synaptic NMDAR-mediated neuroprotection and extrasynaptic NMDAR-mediated neurodegeneration. J. Neurosci. *33*, 18880–18892.
DOI: 10.1523/JNEUROSCI.3293-13.2013

Wang, Y., Zhu, G., Briz, V., Hsu, Y.-T., Bi, X. and Baudry, M. (2014). A molecular brake controls the magnitude of long-term potentiation. *Nature Communications* **5**, Article number: 3051; doi: 10.1038/ ncomms4051.
DOI: 10.1038/ncomms4051

Washio, H., Takigachi-Hayashi, K., and Konishi, S. (1999). Early postnatal development of substantia nigra neurons in rat midbrain slices: hyperpolarization-activated inward current and dopamine-activated current. Neurosci. Res. *34*, 91–101.

Wild, A.R., Akyol, E., Brothwell, S.L.C., Kimkool, P., Skepper, J.N., Gibb, A.J., and Jones, S. (2013). Memantine block depends on agonist presentation at the NMDA receptor in substantia nigra pars compacta dopamine neurones. Neuropharmacology *73*, 138–146.
DOI: 10.1016/j.neuropharm.2013.05.013

Wild, A.R., Jones, S., and Gibb, A.J. (2014). Activity-dependent regulation of NMDA receptors in substantia nigra dopaminergic neurones. J. Physiol. *592*, 653–668.
DOI: 10.1113/jphysiol.2013.267310

Wu, H.-Y., and Lynch, D.R. (2006). Calpain and synaptic function. Mol. Neurobiol. *33*, 215–236.
DOI: 10.1385/MN:33:3:215

Wu, H.-Y., Yuen, E.Y., Lu, Y.-F., Matsushita, M., Matsui, H., Yan, Z., and Tomizawa, K. (2005). Regulation of N-Methyl-D-aspartate Receptors by Calpain in Cortical Neurons. J. Biol. Chem. *280*, 21588–21593.
DOI: 10.1074/jbc.M501603200

Wyllie, D.J.A., Livesey, M.R., and Hardingham, G.E. (2013). Influence of GluN2 subunit identity on NMDA receptor function. Neuropharmacology *74*, 4–17.
DOI: 10.1016/j.neuropharm.2013.01.016

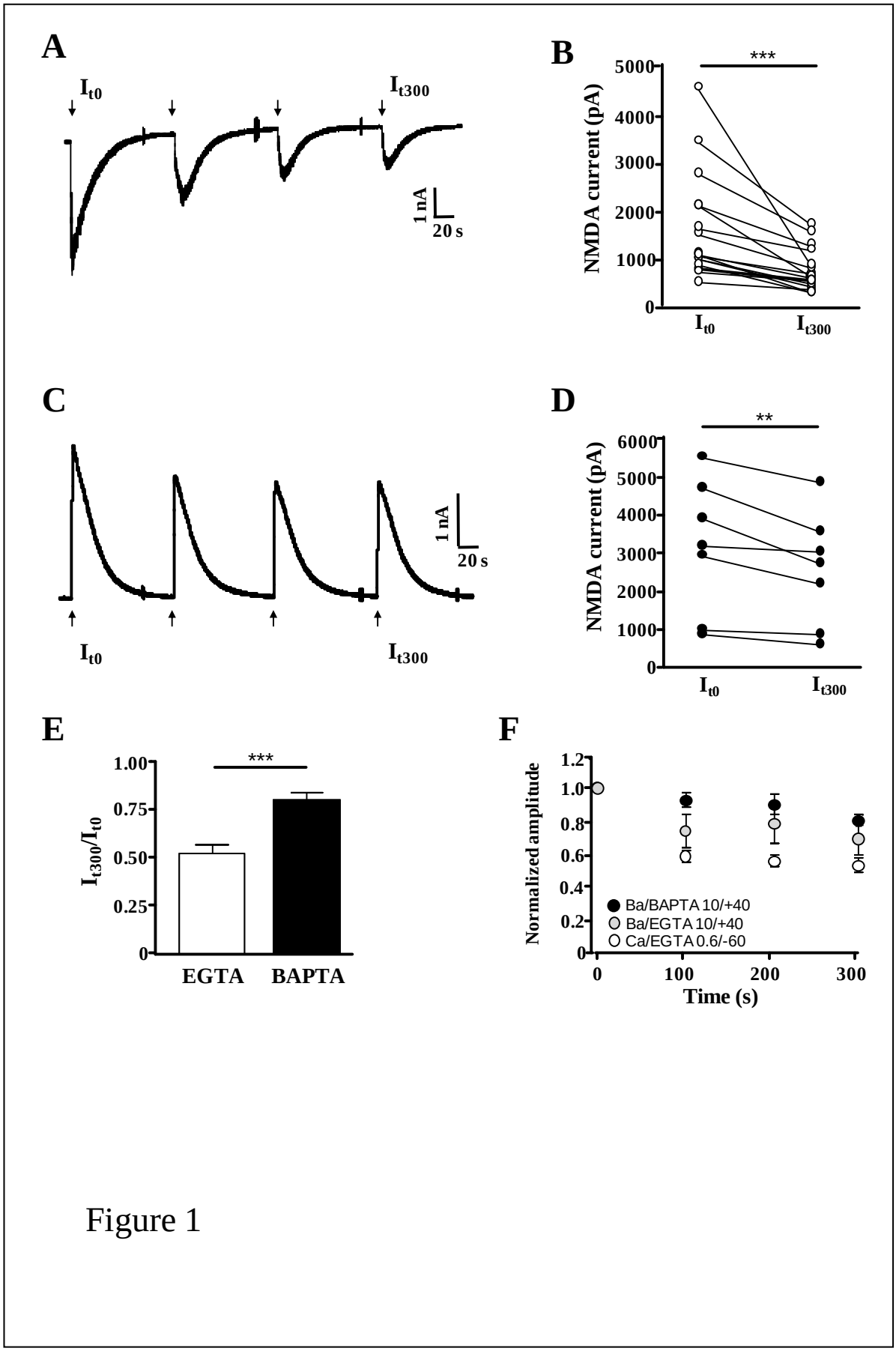
A
I_{t0}
I_{t300}
1 nA
20 s
B
***
NMDA current (pA)
5000
4000
3000
2000
1000
0
I_{t0}
I_{t300}
C
1 nA
20 s
I_{t0}
I_{t300}
D
**
NMDA current (pA)
6000
5000
4000
3000
2000
1000
0
I_{t0}
I_{t300}
E
***
I_{t300}/I_{t0}
1.00
0.75
0.50
0.25
0
EGTA
BAPTA
F
Normalized amplitude
1.2
1.0
0.8
0.6
0.4
0.2
0
Ba/BAPTA 10/+40
Ba/EGTA 10/+40
Ca/EGTA 0.6/-60
0
100
200
300
Time (s)

Figure 1

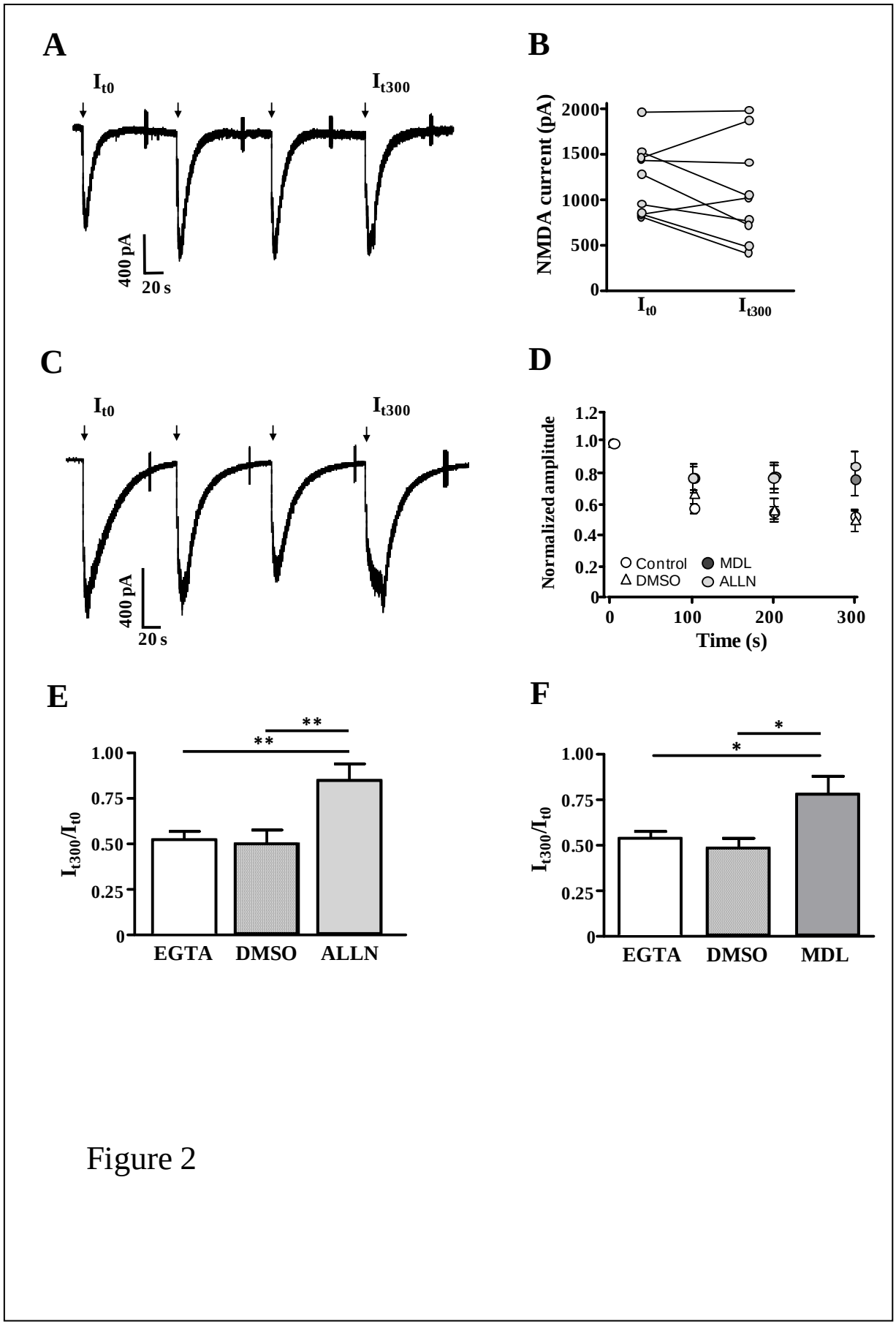
A
I_{t0}
I_{t300}
400 pA
20 s
B
NMDA current (pA)
2000
1500
1000
500
0
I_{t0}
I_{t300}
C
I_{t0}
I_{t300}
400 pA
20 s
D
Normalized amplitude
1.2
1.0
0.8
0.6
0.4
0.2
0
Control
DMSO
MDL
ALLN
0
100
200
300
Time (s)
E
**
**
I_{t300}/I_{t0}
1.00
0.75
0.50
0.25
0
EGTA
DMSO
ALLN
F
*
*
I_{t300}/I_{t0}
1.00
0.75
0.50
0.25
0
EGTA
DMSO
MDL

Figure 2

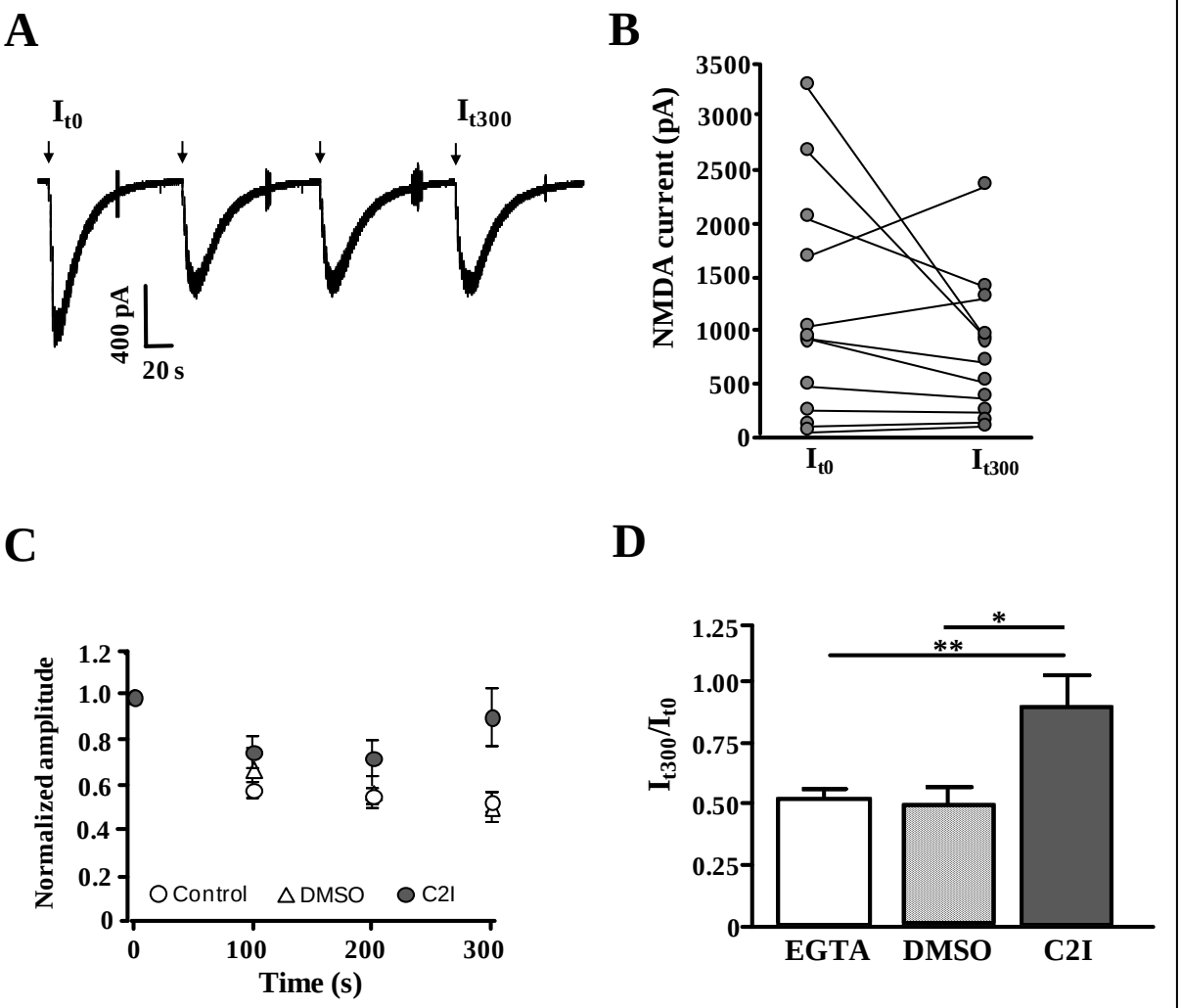
A
I_{t0}
I_{t300}
400 pA
20 s
B
NMDA current (pA)
3500
3000
2500
2000
1500
1000
500
0
I_{t0}
I_{t300}
C
Normalized amplitude
1.2
1.0
0.8
0.6
0.4
0.2
0
Control
DMSO
C2I
0
100
200
300
Time (s)
D
I_{t300}/I_{t0}
1.25
1.00
0.75
0.50
0.25
0
*
**
EGTA
DMSO
C2I

Figure 3

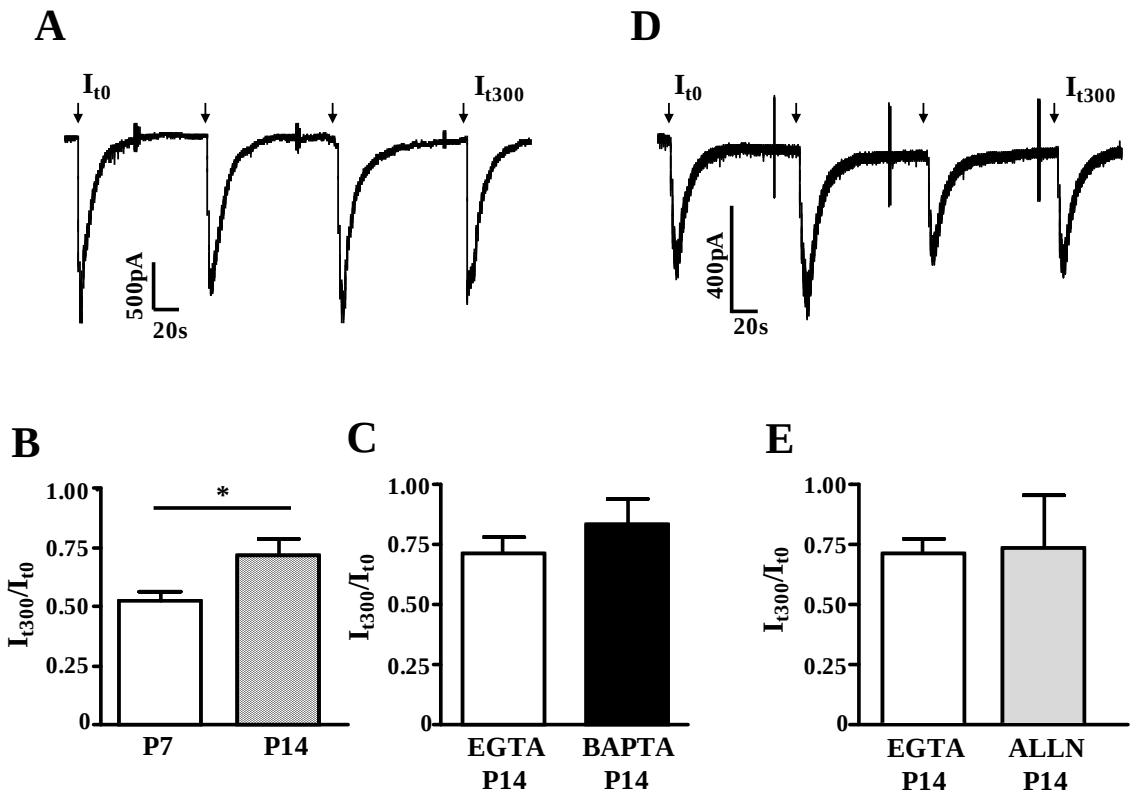
A
I_{t0}
I_{t300}
500pA
20s
D
I_{t0}
I_{t300}
400pA
20s
B
I_{t300}/I_{t0}
1.00
0.75
0.50
0.25
0
*
P7
P14
C
I_{t300}/I_{t0}
1.00
0.75
0.50
0.25
0
EGTA P14
BAPTA P14
E
I_{t300}/I_{t0}
1.00
0.75
0.50
0.25
0
EGTA P14
ALLN P14

Figure 4

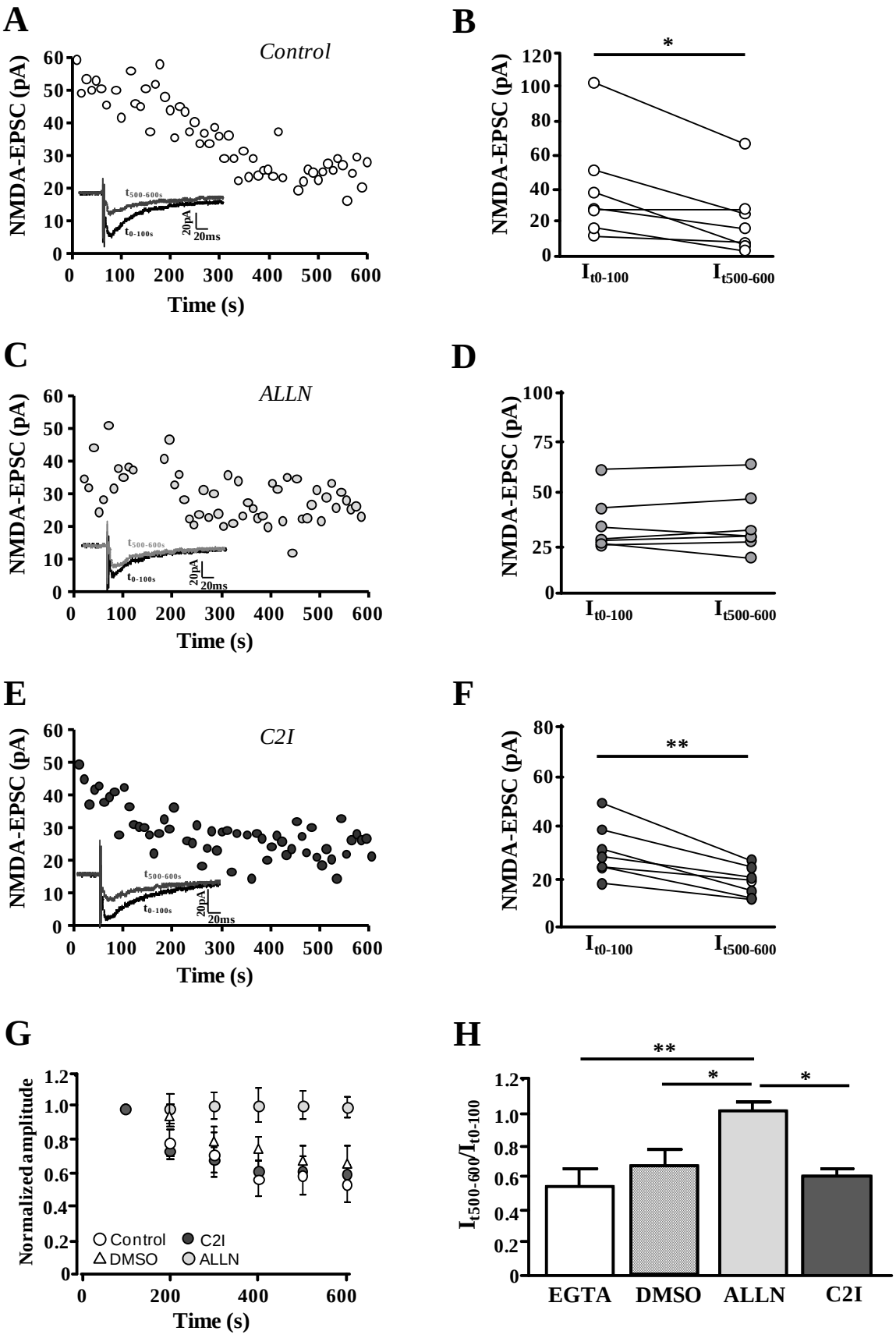
A
Control
NMDA-EPSC (pA)
Time (s)
$t_{500-600s}$
t_{0-100s}
20pA
20ms
B
*
NMDA-EPSC (pA)
I_{t0-100}
$I_{t500-600}$
C
ALLN
NMDA-EPSC (pA)
Time (s)
D
NMDA-EPSC (pA)
I_{t0-100}
$I_{t500-600}$
E
C2I
NMDA-EPSC (pA)
Time (s)
F
**
NMDA-EPSC (pA)
I_{t0-100}
$I_{t500-600}$
G
Normalized amplitude
Control
C2I
DMSO
ALLN
Time (s)
H
**
*
*
$I_{t500-600}/I_{t0-100}$
EGTA
DMSO
ALLN
C2I

Figure 5